Relaxation of Positron Momentum Distribution in Metals*

E. J. Woll, Jr., and J. P. Carbotte
Physics Department, McMaster University, Hamilton, Ontario, Canada
(Received 26 June 1967)

The time-dependent momentum distribution is calculated for positrons, initially of high energy, in contact with a low-temperature electron gas. A Boltzmann-equation approach is used; the positrons are taken to have an effective mass different from the electron mass, as is observed experimentally, and to interact with the electrons via the screened Coulomb interaction. High-momentum components of the distribution decay very quickly; therefore, the Boltzmann equation is solved numerically only for momenta in the thermal range. The distribution function is found to decay with time toward the Maxwell-Boltzmann distribution, while depleting through annihilation. Effective distribution functions, describing the average properties of the positrons throughout the relaxation-annihilation process, are computed for various ratios of lifetime to thermalization time. A prediction is made of the minimum positron energy observable in annihilation experiments.

I. INTRODUCTION

RECENT experiments of Stewart and Shand,[1] of Stewart, Shand, and Kim,[2] and of Kim and Stewart[3] have probed the momentum distribution of positrons annihilating in simple metals at low temperature. Such an experiment was suggested by Majumdar.[4] These experiments demonstrated that over a range of temperatures, the positron was able to come into thermal equilibrium with the electron gas before annihilating, and the analysis showed the positron momentum distribution, if taken to be a Maxwell-Boltzmann distribution for the sample temperature, to correspond to a positron effective mass in the neighborhood of 2 electron masses (from 1.8 for the case of sodium to 2.3 for the case of rubidium).[3]

Early calculations of positron thermalization time by Lee-Whiting[5] suggested that the positron was able to thermalize in times short compared to the positron lifetime. However, recent refinement of the calculation by Carbotte and Arora[6] showed that thermalization time increased sharply as temperature lowered, so that, for low but experimentally realizable temperatures, thermalization time would become comparable to lifetime. The temperature at which this behavior was estimated to occur varied with density. The highest, for simple metals, was for the case of aluminum, where, for temperatures in the neighborhood of 100°K, it was expected that positrons would annihilate before thermalization was complete.

Experimental observation of nonthermalized behavior has been reported by Kim, Stewart, and Carbotte.[7] Effects of nonthermalization were seen at temperatures in the neighborhood of 100°K for sodium and lithium, and of 30°K for rubidium.

It is the purpose of the present paper to consider, in more detail than has been previously reported, the regime in which the positron thermalization time is comparable to its lifetime. To this end, the positron momentum distribution is calculated as a function of time for positrons which lose energy through interaction with the electron gas. A Boltzmann-equation approach is used. This equation is solved numerically for the momentum distribution. The resulting distribution is found to relax with time toward a Maxwell-Boltzmann distribution, while depleting itself through annihilation. Effective momentum distributions are calculated, for various ratios of lifetime to a characteristic thermalization time, (varying with temperature) by suitably averaging over time. It is found, as predicted by Carbotte and Arora[6] and reported by Kim, Stewart, and Carbotte,[7] that positrons annihilate in metals with a certain minimum energy. The value of this energy is predicted for the simple metals.

It should be noted that the Boltzmann equation approach has been used by other authors in the related problem of analyzing properties of positrons annihilating in gases. Application has been made to the problem of positronium formation[8] and to the problem of lifetime[9] in the presence of electric fields. The problem in metals is simpler than that in gases, first, because electric fields are not under consideration, and second, because (for reasons fully discussed in Appendix I) only positron momenta small compared to the Fermi momentum need be considered.

In Sec. II of the present paper the Boltzmann equation for the positron momentum distribution is set up and reduced to a form suitable for computation. In Sec. III, the numerical solution is presented as a universal function of appropriately reduced momentum

* Research supported by the National Research Council of Canada.
[1] A. T. Stewart and J. B. Shand, Phys. Rev. Letters **16**, 261 (1966).
[2] A. T. Stewart, J. B. Shand, and S. M. Kim, Proc. Phys. Soc. (London) **88**, 1001 (1966).
[3] S. M. Kim and A. T. Stewart, Bull. Am. Phys. Soc. **12**, 532 (1967).
[4] C. K. Majumdar, Phys. Rev. **140**, A237 (1965).
[5] G. E. Lee-Whiting, Phys. Rev. **97**, 1157 (1955).
[6] J. P. Carbotte and H. L. Arora, Can. J. Phys. **45**, 387 (1967).
[7] S. M. Kim, A. T. Stewart, and J. P. Carbotte, Phys. Rev. Letters **18**, 385 (1967).
[8] W. B. Teutsch and V. W. Hughes, Phys. Rev. **103**, 1266 (1956).
[9] W. R. Falk, Ph.D. thesis, University of British Columbia, 1965 (unpublished).

and time variables. A discussion of the results is in Sec. IV, with a prediction of the minimum energies observable in annihilation experiments. Two appendices are included. In the first, it is demonstrated that the time development of the momentum distribution is independent of the initial conditions assumed. In the second, a numerical comparison is made with previous work.

II. BOLTZMANN EQUATION

Under the assumption that the positron momentum distribution obeys a Boltzmann equation, the distribution as a function of time is given by[10]

$$\frac{d}{dt}n(\mathbf{p},t)=\sum_{\mathbf{q}}(W(\mathbf{p};\mathbf{q})n(\mathbf{q},t)-W(\mathbf{q};\mathbf{p})n(\mathbf{p},t)) - \frac{1}{\tau_A}n(\mathbf{p},t), \quad (1)$$

where $n(\mathbf{p},t)d^3pdt$ is the probability that, between time t and $t+dt$, a positron will be found having momentum $\hbar\mathbf{p}$ in d^3p. The time τ_A is the lifetime of the positron against annihilatiion, assumed independent of momentum (for the low momenta considered in the present investigation). The function $W(\mathbf{p}';\mathbf{p})$ is the transition probability per unit time for scattering of the positron from state $\mathbf{p}$ to state $\mathbf{p}'$. The sum on $\mathbf{q}$ runs over all states of the positron. Assuming, as is customary,[5,6,11] that the positron is scattered through interaction with the electron gas via the screened Coulomb interaction, it will be adequate to calculate this transition probability in Born approximation. The expression for $W(\mathbf{p}';\mathbf{p})$ is, therefore,[12]

$$W(\mathbf{p}';\mathbf{p})=\frac{4\pi}{\hbar}\sum_{\mathbf{k}}|(\mathbf{k}+\mathbf{p}-\mathbf{p}',\mathbf{p}'|V|\mathbf{k},\mathbf{p})|^2 \times\delta(E^e(\mathbf{k}+\mathbf{p}-\mathbf{p}')+E^p(\mathbf{p}')-E^e(\mathbf{k})-E^p(\mathbf{p})) \times f^+(E^e(\mathbf{k}+\mathbf{p}-\mathbf{p}'))f^-(E^e(\mathbf{k})), \quad (2)$$

where the sum runs over all electron states, labelled by $\mathbf{k}$. The matrix element required is that of the screened Coulomb interaction between an initial state which has a positron of momentum $\hbar\mathbf{p}$ with an electron of momentum $\hbar\mathbf{k}$ and a final state which has a positron of momentum $\hbar\mathbf{p}'$ with an electron of momentum $\hbar(\mathbf{k}+\mathbf{p}-\mathbf{p}')$. The energies $E^e(\mathbf{k})$ and $E^p(\mathbf{p})$ are electron and positron energies, respectively, and are taken to be

$$E^e(\mathbf{k})=\hbar^2k^2/2m, \qquad E^p(\mathbf{p})=\hbar^2p^2/2m^*, \quad (3)$$

where m is the electron mass and m^* is the effective mass of the positron. The functions $f^+(E)$ and $f^-(E)$ are the usual Fermi functions

$$f^-(E)=\{\exp[(E-E_F)/k_B\theta]+1\}^{-1}, \qquad f^+(E)=1-f^-(E), \quad (4)$$

which ensure that the electron scatters from a filled state to an empty state. E_F is the Fermi energy, k_B the Boltzmann constant, and θ the absolute temperature.

In the present calculation, only momentum transfer $\hbar(\mathbf{p}-\mathbf{p}')$ small compared to the Fermi momentum will contribute significantly to the thermalization time. Likewise, the energy transfer in a single scattering will be small compared to the Fermi energy.[13] For these reasons, it will be sufficient to have the matrix elements of the screened potential in the long-wavelength, static limit. Therefore[6]

$$(\mathbf{k}+\mathbf{p}-\mathbf{p}'|V|\mathbf{k},\mathbf{p})=\pi^2e^2a_0/Vk_F \quad (5)$$

will be used, where a_0 is the Bohr radius, V the volume of the crystal, and $\hbar k_F$ is the Fermi momentum.

The distribution function $n(\mathbf{p},t)$ can be written in the form

$$n(\mathbf{p},t)=\exp(-t/\tau_A)f(\mathbf{p},t). \quad (6)$$

The function $f(\mathbf{p},t)$ can be shown by substitution to satisfy an equation like Eq. (1) without the annihilation term $-n(\mathbf{p},t)/\tau_A$. Using an obvious relabelling of momenta with the results of Eqs. (2), (3), and (5), the equation satisfied by $f(\mathbf{p},t)$ can be written

$$\frac{d}{dt}f(\mathbf{p},t) =(4\pi^2e^4a_0^2/\hbar k_F^2V^2)\sum_{\mathbf{k}}\sum_{\mathbf{q}}\delta(E^e(\mathbf{k}+\mathbf{q}-\mathbf{p})+E^p(\mathbf{q}) -E^e(\mathbf{k})-E^p(\mathbf{p}))f^+(E^e(\mathbf{k}))f^-(E^e(\mathbf{k}+\mathbf{p}-\mathbf{q})) \times\{f(\mathbf{q},t)-\exp\{[E^p(\mathbf{p})-E^p(\mathbf{q})]/k_B\theta\}f(\mathbf{p},t)\}, \quad (7)$$

where advantage of the δ-function has been taken to rearrange the Fermi functions slightly. The time-independent solution of Eq. (7) is evidently the Maxwell-Boltzmann (MB) distribution

$$f_B(\mathbf{p})=\eta\exp[-E^p(\mathbf{p})/k_B\theta], \quad (8)$$

where η is a normalizing constant.

[10] R. E. Peierls, *Quantum Theory of Solids* (Clarendon Press, Oxford, England, 1955), p. 127.
[11] S. Kahana, Phys. Rev. **117**, 123 (1960); **129**, 1622 (1963); J. P. Carbotte and S. Kahana, *ibid.* **139**, A213 (1965).
[12] A. Messiah, *Quantum Mechanics* (John Wiley & Sons., Inc., New York, 1965) Vol. II, p. 736.
[13] These matters are discussed in detail by Carbotte and Arora (Ref. 6). The rate of energy loss by the positron is found to be extremely fast until the positron comes near thermal energies, so that, effectively, the whole thermalization time is determined by what happens at thermal energies.

The sums on $\mathbf{k}$ and $\mathbf{q}$ are converted to integrals according to the recipe

$$\sum_{\mathbf{k}} \rightarrow \frac{V}{(2\pi)^3}\int d^3k. \tag{9}$$

The integration on $\mathbf{k}$ can be performed directly, since it involves only known functions. The δ function on energies can be written in terms of momenta as

$$\delta(E^e(\mathbf{k}+\mathbf{q}-\mathbf{p})+E^p(\mathbf{q})-E^e(\mathbf{k})-E^p(\mathbf{p})) = (m/\hbar^2)\delta\{(\mathbf{q}-\mathbf{p})\cdot[\mathbf{k}-\mathbf{p}(m^*+m)/2m^* +\mathbf{q}(m^*-m)2m^*]\}. \tag{10}$$

This δ function confines $\mathbf{k}$ to a plane perpendicular to $\mathbf{q}-\mathbf{p}$. The integration of the Fermi functions over this plane of $\mathbf{k}$ produces the result

$$\int d^3k(m/\hbar^2)\delta[(\mathbf{q}-\mathbf{p})\cdot[\mathbf{k}-\mathbf{p}(m^*+m)/2m^* +\mathbf{q}(m^*-m)/2m^*]\}f^+(E^e(\mathbf{k}))f^-(E^e(\mathbf{k}+\mathbf{q}-\mathbf{p})) = (\pi m^2/m^*\hbar^2)[(q^2-p^2)/|\mathbf{q}-\mathbf{p}|] \times\{1-\exp[(p^2-q^2)/2m^*k_B\theta]\}^{-1}, \tag{11}$$

where terms proportional to $\exp(-E_F/k_B\theta)$ have been neglected.

The integral on angles of $\mathbf{q}$, assuming $f(\mathbf{q},0)$ isotropic, gives the well-known result

$$\int d\Omega_q|\mathbf{q}-\mathbf{p}|^{-1}=4\pi/p, \quad q<p \qquad =4\pi/q, \quad q>p. \tag{12}$$

The final result is an equation for $f(\mathbf{p},t)$ requiring integration only over the magnitude of $\mathbf{q}$, namely,

$$\frac{d}{dt}f(\mathbf{p},t)=(\pi me^4a_0^2/8m^*\hbar E_F)\frac{1}{p}\int_0^p q^2(p^2-q^2)\{1-\exp[(q^2-p^2)/2m^*k_B\theta]\}^{-1}\{\exp[(q^2-p^2)/2m^*k_B\theta]f(\mathbf{q},t)-f(\mathbf{p},t)\}dq + \int_p^\infty q(q^2-p^2)\{1-\exp[(p^2-q^2)/2m^*k_B\theta]\}^{-1}\{f(\mathbf{q},t)-\exp[(p^2-q^2)/2m^*k_B\theta]f(\mathbf{p},t)\}dq. \tag{13}$$

III. COMPUTATION OF DISTRIBUTION FUNCTIONS

For convenience, the dimensionless reduced variables P, Q, and T are defined, where

$$P=p/p_0, \quad Q=q/p_0, \quad T=t/t_0, \tag{14}$$

with

$$\hbar p_0=(2m^*k_B\theta)^{1/2}, \quad t_0=2\hbar E_Fm/\pi m^*(k_B\theta)^2. \tag{15}$$

The function $F(P,T)$ of the reduced variables is defined by

$$F(p/p_0, t/t_0)=(p/p_0)^2f(\mathbf{p},t), \tag{16}$$

and satisfies the equation

$$\frac{d}{dt}F(P,T)=P\Big\{\int_0^P (P^2-Q^2)[1-\exp(Q^2-P^2)]^{-1} \times[\exp(Q^2-P^2)\,F(Q,T)-Q^2F(P,T)/P^2]dQ + \int_P^\infty (Q^2-P^2)[1-\exp(P^2-Q^2]^{-1} \times[PF(Q,T)/Q-\exp(P^2-Q^2) \times QF(P,T)/P]dQ\Big\}. \tag{17}$$

Evidently, the time-independent solution of Eq. (17) is the MB distribution (normalized to 1)

$$F_{\mathrm{MB}}(P)=(4/\sqrt{\pi})P^2\exp(-P^2). \tag{18}$$

Given a starting distribution $F(P,0)$, Eq. (17) determines a universal function $F(P,T)$ of the reduced variables, which relaxes toward the function $F_{\mathrm{MB}}(P)$.

In a physical case, the positrons start from some initial distribution $f(\mathbf{p},0)$, depending on the properties of the β-decay source used, but independent of sample temperature. Since the momentum unit p_0 depends on sample temperature however, the starting distribution $F(P,0)$ should vary with sample temperature. Nevertheless, it is shown in Appendix A that all starting distributions relax, in times negligible compared to thermalization times, to a standard function $F(P,T)$. Therefore, it is unnecessary to use different starting distributions for different temperatures. Moreover, it is not necessary to know the correct starting distribution, since all distributions give the same behavior.

Therefore, for practical purposes, Eq. (17) determines a single universal function of the reduced variables P and T, useful for all temperatures which are low compared to the Fermi temperature.

To find the function $F(P,T)$, Eq. (17) was integrated numerically, using the IBM 7040 computer at McMaster University. Various starting distributions were used in order to check the universality of the function, as discussed in Appendix A. The mesh chosen for momentum integration took P from the values 0 to 8 in steps of 0.2. Time was advanced in increasing steps, according to the formula

$$T=2^{n/8}/1000; \quad n=1, 2, \cdots, 94. \tag{19}$$

The end point 94 was chosen since, at this time, the distribution function was found to be only negligibly different from the MB distribution. The size of the time steps was chosen empirically to assure that the change of $F(P,T)$ in each time step would be small.

Results for $F(P,T)$ are shown in Fig. 1, for a starting distribution

$$F(P,0)=\eta_1 P^2, \quad P<7.8$$
$$=0, \quad P>7.8 \tag{20}$$

(η_1 is a normalizing factor). The function $F(P,T)$ has been plotted for reduced times from 0.002 to 2.048. (Every eighth computed curve has been plotted.) The last curve is for time 3.158, at which time $F(P,T)$ is not distinguishable from the MB distribution, to the scale of the drawing. The time development of $F(P,T)$ is readily apparent from the figure.

Effective distribution functions, suitably averaged over time, have also been computed. For a given reduced positron lifetime T_A, defined by

$$T_A=\tau_A/t_0, \tag{21}$$

the effective distribution function can be defined as the time average of $F(P,T)$ weighted by the factor $\exp(-T/T_A)$ (which gives the depletion of the distribution through annihilation). The result is

$$F_E(P;T_A)\equiv(1/T_A)\int_0^\infty F(P,T)\exp(-T/T_A)dT, \tag{22}$$

which is normalized to 1 if $F(P,T)$ is normalized. For purposes of analysis of experiments, the positron can be taken to annihilate from the momentum distribution $F_E(P;T_A)$.

The functions $F_E(P;T_A)$ were found for various values of T_A by numerically integrating according to Eq. (22), up to the time 3.158. A fraction $\exp(-3.158/T_A)$ of the Boltzmann distribution was added to this result to complete the integral of Eq. (22). The resulting functions $F_E(P;T_A)$ for a number of reduced lifetimes T_A ranging from 0.160 to 10.24 are plotted in Fig. 2. For the largest reduced lifetime plotted, 10.24, $F_E(P;T_A)$ is effectively the Boltzmann distribution (except for a small tail at high momenta reflecting the early history of the positron). For reduced lifetimes comparable to or smaller than 1, $F_E(P;T_A)$ can be seen to differ significantly from the Boltzmann distribution.

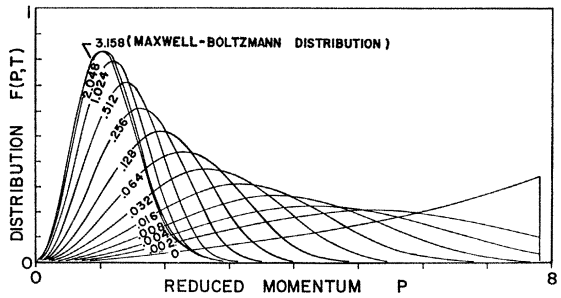

FIG. 1. The positron momentum distribution $F(P,T)$ as a function of reduced momentum P, for various reduced times T. (Curves are labeled by values of the reduced time.) The curve for $T=3.158$ is indistinguishable from the Maxwell-Boltzmann distribution, on the scale of the diagram. Eight curves are computed for every one plotted here.

For a given metal at a given absolute temperature the appropriate T_A, and therefore the corresponding effective distribution of Fig. 2, can be determined from Eqs. (21) and (15). The result is

$$T_A=(\theta/\alpha)^2, \tag{23}$$

with

$$\alpha=(2m\hbar\theta_F/\pi m^* k_B \tau_A)^{1/2}, \tag{24}$$

where θ_F is the Fermi temperature. Values of α for the simple metals are given in Table I.

First and second moments of the distributions have also been computed. For the time-dependent distribution $F(P,T)$, these moments give, respectively, the average momentum and energy of the positron as functions of time. Using the effective distributions $F_E(P;T_A)$, these moments predict the momentum and energy to be observed in annihilation experiments for various values of T_A—that is, for various values of the absolute temperature θ as given by Eq. (23) with Table I.

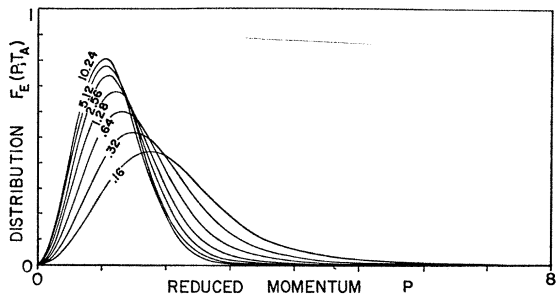

FIG. 2. The effective positron momentum distribution $F_E(P;T_A)$ for various values of the reduced lifetime T_A. Conversion of T_A to temperature for various metals is given by Eq. (23) with Table I.

IV. DISCUSSION

The distribution functions calculated in the present paper are expected, using observed values of the effective mass and positron lifetime, to fit the temperature-dependent behavior observed for two-quantum angular correlation data near the Fermi momentum.[1,2,7] The positron momentum distribution is found to relax to the MB distribution in a few units of reduced time. The time unit t_0 defined in Eq. (14) can therefore be thought of, roughly, as a thermalization time. For low temperatures, this time can become comparable to or larger than the positron lifetime τ_A. (In terms of reduced lifetime: T_A can become of order 1 or smaller.) At such temperatures, the positrons annihilate from an

effective distribution which is broader than the MB distribution appropriate to the sample temperature; significant effects of nonthermalization can, therefore, be expected.

The numerical results of this work can be compared to the results of Carbotte and Arora.[6] Because this comparison is somewhat complicated, it is reserved to Appendix B.

The minimum observable positron energy can readily be calculated, using the effective positron distribution. The positron energy is simply related to the second moment of the effective distribution, by

$$E\equiv\int_0^\infty \frac{\hbar^2p^2}{2m^*}F_E(P;T_A)dP$$

$$=k_B\theta\int_0^\infty P^2F_E(P;T_A)dP. \tag{25}$$

When $F_E(P;T_A)$ approaches the MB distribution

TABLE I. Values of the parameter α which relates the reduced positron lifetime T_A and the absolute temperature θ according to Eq. (23). Values of the Fermi temperature θ_F and the lifetime of the positron against annihilation τ_A are taken from Ref. 4; the effective masses are from Ref. 3.

Metal	θ_F (10^4 °K)	$1/\tau_A$ (10^9/sec)	m^*/m	α (°K)
Cs	1.80	2.4	(2.5)[a]	9.15
Rb	2.09	2.45	3.2	10.4
K	2.39	2.55	2.1	11.8
Na	3.70	3.0	1.8	17.3
Li	5.49	3.5	1.8	12.7
Al	13.5	5.0	(1.8)[a]	42.6

[a] Experimental values of the effective mass are not available; the values used are estimates.

($T_A\gg1$), the average positron energy approaches the value

$$E\underset{T_A\gg1}{\longrightarrow}\tfrac{3}{2}k_B\theta. \tag{26}$$

For values of T_A comparable to or smaller than 1, on the other hand, the energy can be computed using Eq. (25). [The value of T_A is given in terms of θ by Eq. (23) and Table I.] The results are plotted on Fig. 3. For purposes of comparison with the results of Stewart and his collaborators[1,2,7] positron energy is given in terms of "effective positron temperature" θ_E. This temperature is introduced naturally in fitting experimental curves in cases where thermalization is complete before anninilation.[2] In this fitting, the momentum distribution is taken to be a MB distribution for positrons of mass m (rather than m^*) and effective temperature θ_E. Since the MB distribution depends on the product of mass and temperature, the effective positron temperature is given by

$$\theta_E\underset{T_A\gg1}{\longrightarrow}(m^*/m)\theta \tag{27}$$

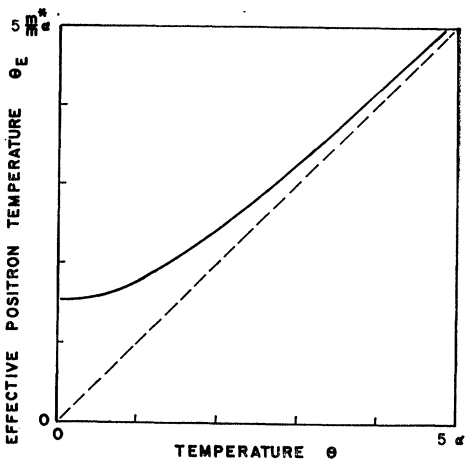

FIG. 3. The positron energy observed in annihilation experiments, expressed as an effective temperature θ_E, as a function of sample temperature. The values of the unit α for the simple metals are given in Table I. This curve is analogous to the experimental curves plotted in Ref. 7. Note that the slope of the dashed line, which would give the positron effective temperature if positrons were able to thermalize, is m^*/m.

in the case where thermalization is complete. In terms of the positron energy, therefore, it can be seen by comparison with Eq. (26) and Eq. (20) that

$$\theta_E=\tfrac{2}{3}(m^*/m)\theta\int_0^\infty P^2F_E(P;T_A)dP. \tag{28}$$

The units of Fig. 3 are given in terms of the quantity α listed, for various metals, in Table I.

The positron can be seen from Fig. 3 to annihilate with a certain minimum effective temperature. The predicted values of this quantity are compared with the measured values in Table II. While the experimental values are expected to be rough, there is a systematic disagreement between them and the theoretical values which is outside the range of reported experimental error, and may be significant. The question of whether a real discrepancy exists must await further experimentation, as well as further theoretical development.

It might be expected that a likely source of error in the treatment of experiment would be the use of a M-B distribution (for an effective positron temperature

TABLE II. A comparison of the predicted and measured values of the minimum effective temperature θ_E. Experimental values are those reported by Kim, Stewart, and Carbotte in Ref. 7.

Metal	Minimum θ_E predicted (°K)	Minimum θ_E measured (°K)
Cs	(36.0)[a]	...
Rb	37.5	~60
K	39.2	~100
Na	49.0	160±50
Li	64.3	~200
Al	(121)[a]	...

[a] Unknown effective masses have been estimated to produce these results. See Table I.

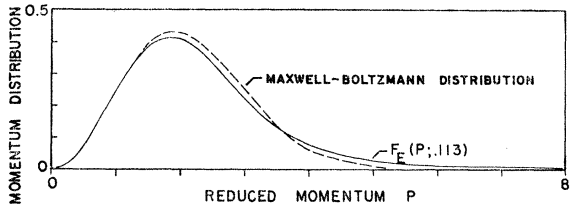

FIG. 4. A comparison of the effective momentum distribution for reduced lifetime $T_A=0.113$ with a Maxwell-Boltzmann distribution chosen so that both curves have maxima at the same value of P. The two curves correspond to effective positron temperature different by about 10%, as discussed in Sec. IV.

θ_E' *different* from $m^*\theta/m$) to describe the positron in fitting experimental data in cases where the positron is not thermalized. The general magnitude of error introduced by this procedure can be estimated by comparing a M-B distribution to the calculated effective distribution. In Fig. 4, the effective distribution for reduced lifetime $T_A=0.113$ has been plotted as a solid line. The dashed line on the same figure is a MB distribution chosen to peak at the same momentum, $P=1.92$. This distribution corresponds to an effective positron temperature θ_E' of

$$\theta_E'=(1.92)^{1/2}m^*\theta/m \\ =1.38m^*\theta/m. \quad (29)$$

The value of the positron energy in the calculated effective distribution, in terms of effective positron temperature, is computed from Eq. (28) to be

$$\theta_E=1.53m^*\theta/m. \quad (30)$$

The discrepancy in these two values is about 10%; presumably, errors of this order can be expected if a MB distribution is used to approximate the effective positron distribution. It should be noted that choosing a MB distribution which peaks at the same value as the effective distribution does not necessarily match the curve fitting procedure actually used.[1,2,7] The 10% estimate made here should, therefore, be considered only indicative of the error to be expected.

Finally, it should be noted that the present calculation does not include effects of a possible variation of enhancement factor with positron momentum. Since the enhancement factor is known to be a rapidly varying function of electron momentum near the Fermi momentum,[14] its behavior as a function of positron momentum is certainly worth investigating. This investigation should not affect the theoretical results of the present work, but could be of some importance in application to the analysis of experiments.

ACKNOWLEDGMENTS

The authors are grateful to Professor A. T. Stewart and Professor S. Berko for stimulating discussions. In addition, Professor Garth Jones is to be thanked for providing information concerning the related problem of positron diffusion in gases.

[14] J. P. Carbotte, Phys. Rev. **155**, 197 (1967).

APPENDIX A

The argument that the results of the present paper are independent of starting distribution requires two steps. First it must be shown that, for momenta outside the computed range 0 to 8 momentum units, the distribution falls to zero in times short compared to the smallest time steps used. This fact justifies the choice of a starting distribution confined to the range 0 to 8. Second, it must be shown that the details of shape of the starting distribution within the range 0 to 8 do not matter; that is, that all distributions produce identical results after times small compared to thermalization time.

The range of validity of Eq. (13) or Eq. (17) for the distribution function is limited to momenta small compared to the Fermi momentum, for several reasons: first, because the screened Coulomb potential has been approximated by its static long-wavelength limit. This neglects the momentum dependence which appears for momenta comparable to $\hbar k_F$ but, more importantly, neglects the coupling to the plasma oscillations of the electron gas. Also, at momenta comparable to $\hbar k_F$, the

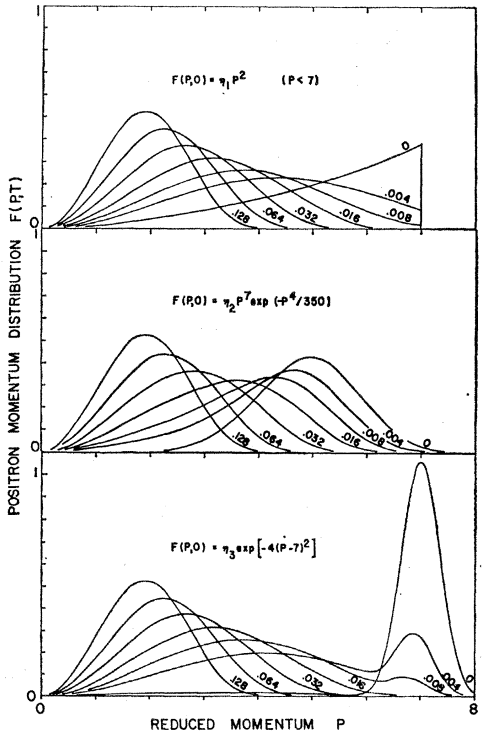

FIG. 5. The time development from differently shaped starting distributions is compared. After 0.064 time units, these curves differ by less than 10% at all mesh points. (Thermalization time is about 2 time units.) Development after 0.128 time units is the same for all starting distributions; identical to that shown on Fig. 1.

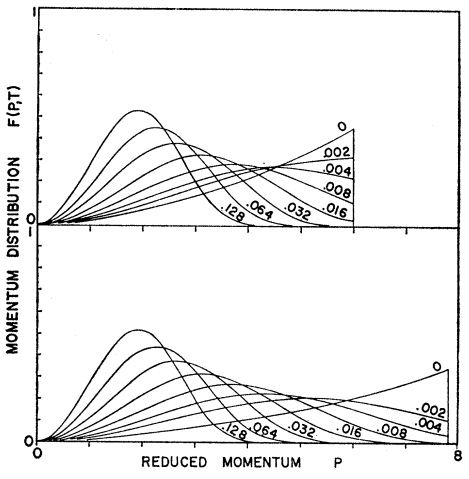

FIG. 6. The time development from two starting distributions of different extension along the P axis. Use of these different distributions would be appropriate for two temperatures θ_1 and θ_2 whose ratio was $\theta_1/\theta_2=0.63$. After 0.064 time units (thermalization time is about 2 time units) the difference between the two distributions is within 10% at all mesh points.

phase space available for the positron scattering is different from that given in Eq. (11). However, for $P\gg1$, the logarithmic derivative of $F(P,T)$ will monotonically increase with P [though not necessarily so fast as Eq. (17) would predict]. It is therefore possible to consider momenta near $P=8$, when Eq. (17) is valid, in order to put an upper limit on decay time for the distribution for all higher momenta. For $P\sim8$, the thermal factors in Eq. (17) ensure that the scattering-in term will make no contribution to $(d/dt)F(P,T)$. Equation (17) then reduces to the form

$$\frac{d}{dt}F(P,T)\underset{P\gg1}{\longrightarrow}-\frac{1}{P}\int_0^P Q^2(P^2-Q^2)dQF(P,T)$$
$$=-(2P^4/15)F(P,T). \quad \text{(A1)}$$

This equation can be integrated directly to give

$$F(P,T)\underset{P\gg1}{\longrightarrow}F(P,0)\exp(-2P^4T/15). \quad \text{(A2)}$$

This dependence can easily be checked in the numerical results for $P=7$, for example. For momenta of 8 or higher, the coefficient of T in the exponent of Eq. (A2) is greater than 546. The characteristic time for decay of the function for such momenta is therefore smaller than 0.0018 time units; comparable to the smallest time steps considered in the present work. Therefore, it is justified to use a starting distribution confined to momenta smaller than 8.

However, the shape of the distribution, while known to be confined, is not known for the earliest times, and results might be expected to depend on the details of this shape. In order to answer this question, $F(P,T)$ was computed for a selection of different initial distributions. The time development of three different distributions is shown in Fig. 5. The result is that all distributions agree within 10% for all mesh points at reduced times $T>0.064$, and that agreement is essentially complete at 0.128 time units. The time development of two distributions which are the same except for a scaling factor on the P axis was also investigated. (This corresponds to using the *same* distribution $f(\mathbf{p},0)$ with two different sample temperatures, which would be expected physically to be the right procedure.) The results are plotted in Fig. 6. Evidently, agreement is reached here as quickly as in the cases plotted in Fig. 5.

The conclusion is that the nature of the starting distribution does not significantly affect the results reported.

APPENDIX B

Comparison of the present results with those of Lee-Whiting[5] and of Carbotte and Arora[6] is not completely straightforward. These authors calculate thermalization times according to the following prescription: at any time, the positron is imagined to be in a single, well-defined momentum state. The rate of energy loss for the positron in contact with a zero-temperature electron gas is then calculated from the transition probability. The positron is then taken to lose energy at the calculated rate, successively passing through well-defined states until it reaches thermal energies. The rate of change of energy, calculated as described, is

$$\frac{d}{dt}E^p(\mathbf{p})=\frac{4\pi}{h}\sum_{\mathbf{q}}W(\mathbf{q};\mathbf{p})(E^p(\mathbf{q})-E^p(\mathbf{p})), \quad \text{(B1)}$$

when the transition probability $W(\mathbf{q};\mathbf{p})$ and the positron energies are defined in Sec. II, but taken in the zero-temperature limit (so that Fermi functions are replaced by step functions). Using the assumptions of Sec. II, the sum on $\mathbf{q}$ can be readily performed. The result is

$$\frac{d}{dt}E_{CA}=-(8/105)(\pi m^*/2mhE_F)E_{CA}^3, \quad \text{(B2)}$$

where E_{CA} has been written for the positron energy calculated in this manner. The Eq. (B2) can be directly integrated to give

$$E_{CA}^2=(105/16)(2\hbar E_F m/\pi m^*)/t. \quad \text{(B3)}$$

This result agrees with the prediction of Carbotte and Arora[6] (generalized to take account of the positron effective mass). The dependence indicated by Eq. (B3) is plotted as a dashed line on Fig. 7.

However, the energy-loss process for the positron is inherently statistical. Properly, therefore, it should be imagined that the initial positron state decays (with probability given by the Fermi golden rule) into a number of possible states. The energy of the positron should then be evaluated as an average over all states.

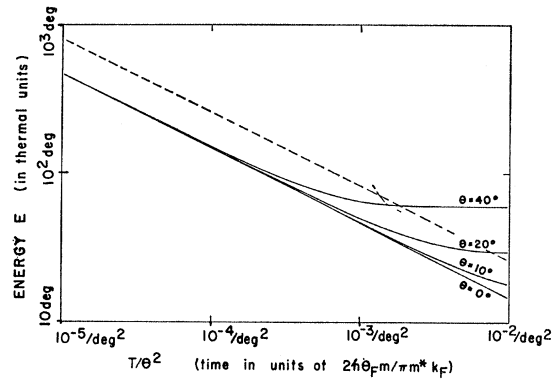

FIG. 7. The average positron energy as a function of time for various absolute temperatures. Note that both scales are logarithmic. The unit for the time axis has the value $\alpha^2\tau_A$, whose values are given in Table I. The dashed curve is the prediction of Carbotte and Arora in Ref. 6. Note that the solid curve corresponds to the curve sketched by Stewart, Shand, and Kim in Ref. 2.

In the language of the present paper, the positron energy should be defined as an average over the distribution function $F(P,T)$,

$$E=\int_0^\infty (\hbar^2p^2/2m^*)F(P,T)dP$$

$$=k_B\theta\int_0^\infty P^2F(P,T)dP. \tag{B4}$$

This energy can easily be computed as a function of reduced time, using the distributions found in Sec. III. The result is plotted in Fig. 7. The dependence of E on T as displayed is quite interesting. First, the dependence on absolute temperature, which might be expected from Eq. (B4) to be strong, is, in fact, nonexistent until the energy reaches values near the thermal value $\frac{3}{2}k_B\theta$. Second, for energies appreciably larger than $\frac{3}{2}k_B\theta$, the curves have a dependence which, except for the constant of proportionality between E^2 and $1/T$, is identical to that predicted by Carbotte and Arora. Since for smaller and smaller θ the energy drops lower and lower before flattening out, the straight line on Fig. 7 must be the true E-versus-T curve for the case of zero temperature. Note that this curve is similar to the curve sketched by Stewart, Shand, and Kim.[2]

The behavior of E with T can be understood, and the discrepancy with Carbotte and Arora in the proportionality constant can be resolved, by computing the rate of energy loss directly. Time differentiation of Eq. (B4) gives

$$\frac{d}{dt}E=k_B\theta\int_0^\infty P^2\frac{d}{dt}F(P,T)dP. \tag{B5}$$

The rate of change of $F(P,T)$ can be evaluated using Eq. (17). [In the limit of low temperatures, the exponential factors in Eq. (17) are identically zero.] The result, for low temperatures, is

$$\frac{d}{dt}E=k_B\theta\Big[-\int_0^\infty PF(P,T)\int_0^P Q^2(P^2-Q^2)dQdP$$

$$+\int_0^\infty P\int_P^\infty 1/Q(Q^2-P^2)F(Q,T)dQdP\Big]$$

$$=k_B\theta\int_0^\infty F(P,T)\Big[-P\int_0^P Q^2(P^2-Q^2)dQ$$

$$+1/P\int_P^\infty Q(P^2-Q^2)dQ\Big], \tag{B6}$$

after making suitable rearrangements of limits and integration variables. The result is

$$\frac{d}{dt}E=-(8k_B\theta/105)\int_0^\infty P^6F(P,T)dP. \tag{B7}$$

By dimensional arguments, it can be expected that

$$\int_0^\infty P^6F(P,T)dP=A(E/k_B\theta)^3. \tag{B8}$$

In this event

$$\frac{d}{dt}E=-(8A/105)E^3/(k_B\theta)^2. \tag{B9}$$

This equation can be integrated to give

$$E^2=(105/16A)(k_B\theta)^2/T, \tag{B10}$$

where the (presumed) constant A is a geometrical property of the distribution $F(P,T)$. In Table III values of A are given for various times T, computed using the distribution shown in Fig. 1. The constancy of A is thereby established by direct calculation, and its value is found to be 2.70.

TABLE III. Values of the second and sixth moments $\langle P^2\rangle$ and $\langle P^6\rangle$ and of the parameter A, calculated for four different reduced times. The parameter is seen to be constant for these reduced times (small compared to thermalization time).

T	$\langle P^2\rangle$	$\langle P^6\rangle$	A
0.032	8.32	559	2.70
0.064	5.94	564	2.70
0.128	4.24	205	2.70
0.256	3.05	77.0	2.71

The Carbotte-Arora result can be seen by comparison of Eq. (B10) with Eq. (B3), taking account of the time unit given in Eq. (15), to correspond to the value $A=1$. This is just the value which would be obtained if $F(P,T)$ were at all times a δ function in momentum. This fact

therefore sheds light on the assumption that the positron's energy can be calculated as though it were always in a single state: that assumption *overestimates* the coefficient of the E^2-versus-$1/T$ curve by a factor 2.70, thereby *underestimating* the rate at which energy is lost.

For purposes of comparison, it is instructive to compute the value A would have if $F(P,T)$ were at all times a MB distribution corresponding to some temperature θ' higher than the sample temperature θ. In this case

$$F(P,T)=(4/\sqrt{\pi})(\theta/\theta')^{3/2}P^2\exp(-P^2\theta/\theta')$$

$$\int_0^\infty P^6F(P,T)=(\theta'/\theta)^3 3\times5\times(\tfrac{7}{2})^3 \qquad \text{(B11)}$$

$$\int_0^\infty P^2F(P,T)=(\theta'/\theta)^{\frac{3}{2}},$$

yielding

$$A=5\times(\tfrac{7}{2})=3.889. \qquad \text{(B12)}$$

If it were true, therefore, that the positron distribution was a M-B distribution for an effective temperature varying with time, the factor of disagreement between the present calculation and the calculation of Carbotte and Arora would *increase*.

The basis of the surprisingly large disagreement as to the value of the factor A in different distributions is the fact that A depends on the sixth moment of the distribution. It should be emphasized, however, that effective temperatures are estimated by setting $E(T_A)=\frac{3}{2}k\theta$. The estimated temperature therefore depends on the square root of the coefficient A. The factor of disagreement in the effective temperature is therefore $\sqrt{(2.70)}=1.64$. This factor is roughly compensated for by the effective-mass factor, so that the present predictions are close to those of Carbotte and Arora.

PHYSICAL REVIEW VOLUME 164, NUMBER 3 15 DECEMBER 1967

Modifications to the Orthogonalized-Plane-Wave Method for Use in Transition Metals: Electronic Band Structure of Niobium*

R. A. DEEGAN† AND W. D. TWOSE‡
Department of Physics, McMaster University, Hamilton, Ontario, Canada
(Received 10 July 1967)

Modifications to the orthogonalized-plane-wave (OPW) method are employed to facilitate its application to transition metals. The procedure is to augment the basis set of OPW's by including functions which vanish in the interstitial regions of the crystal but represent well the outer core functions and the d-band states near the nuclei. The bands are found to converge at a rate approximately the same as for the unmodified OPW method in semiconductors. The method is applied to calculate the conduction electron bands of niobium, along principal symmetry directions, to a convergence of about 0.01 Ry. The resulting band structure is very similar to previous augmented-plane-wave calculations for other bcc transition metals.

1. INTRODUCTION

THIS paper presents a method for calculating the electronic band structures of transition metals, based on modifications to the orthogonalized-plane-wave method. The modified method is applied to the transition metal niobium, for which convergence of the bands to about 0.01 Ry is obtained.

Difficulties in applying the OPW method to transition metals arise from: (1) the slow convergence for d-like conduction states[1]; and (2) the fact that the outermost s and p core states[2] are not completely localized but form bands of nonzero width. Problem (1) occurs because the wave function of a d state is not well represented by the $l=2$ component of a plane wave, even if the latter has been orthogonalized to a core level of d character. Problem (2) prevents orthogonalization of the plane waves to the outer core levels in the usual manner.

Following a suggestion by Herring,[3] which was later used by Callaway,[4] the d-band convergence is improved by adding to the basis set of OPW's a function which represents well the behavior of the d conduction band states in the inner region of the core but which is chosen to vanish in the interstitial regions. Similar cutoff (CO) functions are added to the basis set to represent the behavior of the outer core s- and p-wave functions, while the plane waves are orthogonalized to only those

* Based on a thesis submitted by R. A. D. in partial fulfilment of the requirements for the Ph.D. degree. This work was financially supported in part by the National Research Council of Canada.
† Present address: Cavendish Laboratory, University of Cambridge, Free School Lane, Cambridge, England.
‡ Dr. Twose died on April 5, 1967.
[1] Herman found that, for the $\Gamma_{25'}$ (d-like) state in diamond, a 16th order reduced secular equation (296 OPW's) was required to give the energy to within a few percent of convergence: F. Herman, Phys. Rev. **93**, 1214 (1954).
[2] Throughout this paper the term *core states* is used to designate the corelike eigenfunctions of the one-electron conduction band crystal Hamiltonian.
[3] C. Herring, Phys. Rev. **57**, 1169 (1940).
[4] J. Callaway, Phys. Rev. **97**, 933 (1955); **99**, 500 (1955).